A Tightly Coupled Positioning Method of Ranging Signal and IMU Based on NLOS Recognition

1st Ke Han
Institute of Electronic Engineering
Beijing University of Posts and Telecommunications
Beijing, China
hanke@bupt.edu.cn

2st Bingxun Liu
Institute of Electronic Engineering
Beijing University of Posts and Telecommunications
Beijing, China
liubingxun@bupt.edu.cn

3st Zhongliang Deng
Institute of Electronic Engineering
Beijing University of Posts and Telecommunications
Beijing, China
dengzhl@bupt.edu.cn

***Abstract*—Due to the complex indoor environment, the human body and infrastructure will cause the non-line-of-sight (NLOS) error, resulting in inaccurate ranging information. To effectively use the inertial measurement unit (IMU) to reduce the NLOS error, a tightly coupled localization method based on NLOS signal adaptive recognition is proposed in this paper. Firstly, the method predicts the distance from the base station to terminals using the tight coupling of the IMU and the ranging signal. Secondly, we propose an NLOS recognition method based on the residuals between the observed and predicted values of distance. In the form of a sliding window, the residuals are clustered using a Gaussian mixture model (GMM), and the clustering results are optimized by introducing the concept of time series. The NLOS recognition is made according to the obtained residual distribution model. Then, the error state Kalman filter (ESKF) is performed on the residuals identified as line-of-sight (LOS) to correct the position information of the terminal. Simulation results show that this recognition method has higher sensitivity and accuracy. We also use ultra-wideband (UWB) to test. The results show that in the mixed environment of LOS and NLOS, this method can identify Los signals and use them for positioning, and the accuracy is 47% higher than traditional tight coupling.**

Keywords—tightly coupled, non-line-of-sight, IMU, GMM, Error State Kalman filter

I. INTRODUCTION

In recent years, location-based services (LBS) have been widely used in both civil and military fields. Especially with the rise of the Internet of things and the construction of the smart city, the importance of spatial geographic information with positioning and navigation as the main service content is more prominent. In outdoor positioning scenarios, using satellite positioning functions, countries have built global navigation satellite systems (GNSS) such as GPS, Beidou, GLONASS, and Galileo. These positioning systems are becoming more and more perfect in people's daily use. With the rapid advancement of urbanization today, people spend more than 80% of their time indoors, and people put forward more demands for indoor LBS [1]. Due to the shielding and reflection of walls in the indoor environment, it is difficult for satellite signals to achieve an ideal positioning effect. A large number of indoor positioning technologies, such as UWB, Bluetooth, radio frequency identification (RFID), Wi-Fi, and inertial navigation system (INS), have been gradually applied to all walks of life. These technologies use time-of-arrival (TOA), time-difference-of-arrival (TDOA), received signal strength indication (RSSI), angle of arrival (AOA), and other methods. Compared with other technologies, UWB has better penetration. It has strong permeability and anti-multipath interference ability, so it is more suitable for indoor positioning [2]. In terms of the positioning error, the positioning results of UWB technology are unstable in adjacent time, but the error will not increase significantly with time. The inertial navigation system based on sensing elements is relatively stable in positioning results in a short time, however, the errors of inertial measurement elements will gradually accumulate over time. Combining the two can make up for their defects, reduce errors and enhance the accuracy and reliability of positioning.

The complex indoor environment makes positioning methods often face the influence of NLOS propagation, resulting in a decrease in positioning accuracy [3]. Many scholars have studied how to reduce NLOS error. The residual weighting algorithm (RWGH) is a classical algorithm. By weighting different combinations of range measurement, the effect of NLOS can be reduced [4]. Wang proposed a non-closure checking algorithm for NLOS environments where anchor nodes are sparse. The algorithm obtains possible NLOS measurements from the wrong closures of different triangles by checking them [5]. Q. Shi considers using IMU to determine the position of the UWB anchor node, and tightly couples IMU and UWB by using the error state Kalman filter. The root mean square error (RMSE) of the anchor node position obtained by the experiment is less than 0.1 meters [6]. Z. Zeng proposed to use UWB channel impulse response (CIR) for NLOS detection, conduct preliminary UWB ranging value screening, and fuse IMU and the filtered UWB ranging value through extended Kalman, to achieve better position estimation under NLOS conditions [7]. Wang Y uses the particle filter to fuse IMU and UWB. The prior information is provided by IMU. The weight update is based on the observation value of UWB. Under the condition of NLOS, the positioning error is reduced and the calculation resource consumption is small, which is suitable for embedded devices [8]. L. Cheng uses the k-means clustering algorithm to identify and eliminate the measured values under NLOS conditions to improve the accuracy of the measured distances [9]. F. Wu uses the difference between the asymmetric two-way ranging information and the INS information as the measurement information, respectively assigns weights to remove outliers, and uses the Kalman filter for downhole positioning and attitude angle calculation. Compared with the original IMU and UWB fusion, this method is more suitable for the localization environment in the mine [10]. Although many scholars have studied NLOS error, due to its complexity, NLOS is still one of the key issues affecting indoor positioning accuracy.

Considering that tight coupling is better than loose coupling, this paper combines UWB and IMU with tight coupling. We propose an NLOS recognition method based on clustering algorithm, and then use the recognition results for tight coupling. Firstly, the method uses the IMU to predict the distance from the base station to the terminal and obtains the

978-1-7281-6218-8/22/$31.00 ©2022 IEEE

2022 IEEE 12th International Conference on Indoor Positioning and Indoor Navigation (IPIN) | 978-1-7281-6218-8/22/$31.00 ©2022 IEEE | DOI: 10.1109/IPIN54987.2022.9918144

residual between the predicted value and the observed value. Secondly, we use a sliding window to retain the past residuals and perform GMM clustering on the residuals. After clustering, The algorithm introduces a time decay factor to optimize the clustering results, obtains the Gaussian model of residual distribution, and performs NLOS recognition according to the model. Then, ESKF is performed on the difference value identified as LOS to correct the position information of the terminal. In addition, the measurement noise variance of the filter is also modified according to the residual distribution.

The rest of this paper is organized as follows. Section II introduces the theory of UWB and INV, as well as the theory of tight coupling based on ESKF. Section III introduces the composition of NLOS signals and proposes an NLOS recognition method based on clustering. Section IV describes the framework of our proposed method. In Section V, we test the localization method in a real environment and analyze the experimental results. Finally, we give conclusions in Section VI.

II. Tight Coupling of UWB and IMU

UWB signal is a kind of non-sinusoidal extremely narrow pulse signal, which has the characteristics of high time resolution, strong penetration and low power consumption, and is widely used in the field of indoor positioning. Its ranging methods mainly include two-sided two-way ranging. Compared with other indoor positioning technologies, UWB has the advantages of higher accuracy and stability in positioning [11]. After collecting the distance measurements from the target terminal to each base station, the terminal location is calculated from the base station location. Solutions can be TOA or TDOA. TOA is often solved by the least squares method. Common TDOA algorithms include the Fang algorithm, Chan algorithm, Taylor algorithm, and least squares algorithm [12].

INS is a classic indoor positioning method. The IMU consists of gyroscopes and accelerometers, which obtain angular velocity and acceleration information of the object, and uses integral operations to calculate the current position and posture of the object. The IMU has the advantage of data update rate, continuous posture and location information, and no environmental impact. It can provide continuous attitude and position information and is not affected by the external environment. The disadvantage is that the positioning error accumulates continuously during the integration process, so it is not suitable for long-term independent use.

There are usually two combinations of UWB and IMU, loose coupling and tight coupling. The loose coupling method is relatively simple. Each positioning system carries out an independent positioning solution and modifies the positioning results. The tight coupling method is relatively complex. It can correct the observed quantities and some parameters of each system. When the number of ranging values is less than the solution requirement, the loose coupling will fail, but the tight coupling can still work. Tight coupling usually improves positioning accuracy better than loose coupling.

The positioning principle of tight coupling between UWB and IMU is shown in Figure 1.

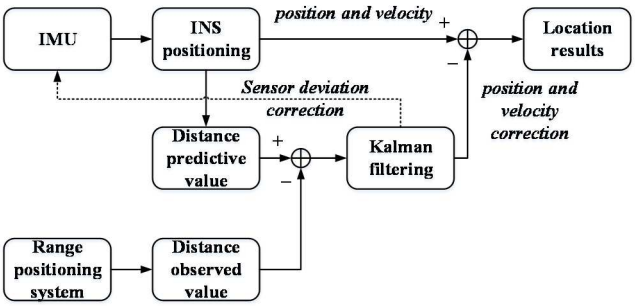

Fig. 1. Tight coupling model

ESKF is more suitable for INS than the classical Kalman filter [13]. When using ESKF, the state vector is described as

$$\boldsymbol{x} = [\boldsymbol{p} \quad \boldsymbol{v} \quad \boldsymbol{q} \quad \boldsymbol{a}_b \quad \boldsymbol{\omega}_b]^T \tag{1}$$

where $\boldsymbol{p}$ is the position of the target terminal, $\boldsymbol{v}$ is the speed of the terminal, $\boldsymbol{q}$ is the attitude of the terminal expressed in quaternion, $\boldsymbol{a}_b$ is the deviation of acceleration, and $\boldsymbol{\omega}_b$ is the deviation of angular velocity. The state before filtering is called the nominal state.

Assuming that the measurement distance from each base station to the terminal is $d_i(t)$, the observation vector can be described as

$$\boldsymbol{y} = [d_1(t) \quad d_2(t) \quad ...]^T \tag{2}$$

The error state vector is described as

$$\delta\boldsymbol{x} = [\delta\boldsymbol{p} \quad \delta\boldsymbol{v} \quad \delta\boldsymbol{\theta} \quad \delta\boldsymbol{a}_b \quad \delta\boldsymbol{\omega}_b]^T \tag{3}$$

In (3), $\delta\boldsymbol{\theta}$ represents the attitude error in the form of an angle, which is different from the quaternion in the nominal state.

The filtered state is called the truth state, denoted as $\boldsymbol{x}_t$. The true state is defined as the sum of the nominal state and the error state.

$$\boldsymbol{x}_t = \begin{bmatrix} \boldsymbol{p}_t \\ \boldsymbol{v}_t \\ \boldsymbol{q}_t \\ \boldsymbol{a}_{bt} \\ \boldsymbol{\omega}_{bt} \end{bmatrix} = \begin{bmatrix} \boldsymbol{p} + \delta\boldsymbol{p} \\ \boldsymbol{v} + \delta\boldsymbol{v} \\ \boldsymbol{q} \otimes \delta\boldsymbol{\theta} \\ \boldsymbol{a}_b + \delta\boldsymbol{a}_b \\ \boldsymbol{\omega}_b + \delta\boldsymbol{\omega}_b \end{bmatrix} = \boldsymbol{x} + \delta\boldsymbol{x} \tag{4}$$

ESKF predicts and corrects $\delta\boldsymbol{x}$. The prediction equation is as (5),

$$\delta\boldsymbol{x} \leftarrow \boldsymbol{F}_{\boldsymbol{x}} \cdot \delta\boldsymbol{x} \tag{5}$$

where, $\boldsymbol{F}_{\boldsymbol{x}}$ is the Jacobian matrix obtained by the partial derivative of the state transition function $f(\boldsymbol{x}, \delta\boldsymbol{x}, \boldsymbol{u}_m, \boldsymbol{i})$ to $\delta\boldsymbol{x}$, $\boldsymbol{F}_{\boldsymbol{i}}$ is the noise transfer matrix, $\boldsymbol{u}_m$ is the input vector and $\boldsymbol{i}$ is the state transition noise.

Assuming that the time interval of the update process is Δt, the acceleration obtained by the IMU is $\boldsymbol{a}_m$, the angular velocity obtained by the IMU is $\boldsymbol{\omega}_m$, the rotation matrix is $\boldsymbol{R}$, and the gravitational acceleration is $\boldsymbol{g}$, then the nominal state update equation of the prediction process is

$$\begin{aligned} \boldsymbol{p} &\leftarrow \boldsymbol{p} + \boldsymbol{v}\Delta t + \frac{1}{2}(\boldsymbol{R}(\boldsymbol{a}_m - \boldsymbol{a}_b) + \boldsymbol{g})\Delta t^2 \\ \boldsymbol{v} &\leftarrow \boldsymbol{v} + (\boldsymbol{R}(\boldsymbol{a}_m - \boldsymbol{a}_b) + \boldsymbol{g})\Delta t \\ \boldsymbol{q} &\leftarrow \boldsymbol{q} \otimes \boldsymbol{q}(\boldsymbol{\omega}_m - \boldsymbol{\omega}_b)\Delta t \\ \boldsymbol{a}_b &\leftarrow \boldsymbol{a}_b \\ \boldsymbol{\omega}_b &\leftarrow \boldsymbol{\omega}_b \end{aligned} \tag{6}$$

We define $\boldsymbol{Q}$ as the process noise covariance matrix and $\boldsymbol{R}$ as the observation noise covariance matrix.

The error state covariance updating equation of the prediction process is

$$\boldsymbol{P} \leftarrow \boldsymbol{F_x P F_x^T} + \boldsymbol{F_i Q F_i^T} \tag{7}$$

The Kalman gain is expressed as

$$\boldsymbol{K} = \boldsymbol{P H^T (H P H^T + R)^{-1}} \tag{8}$$

where $\boldsymbol{H}$ is obtained from the partial derivative of $\boldsymbol{x}$ by the observation function $h(\boldsymbol{x}, \boldsymbol{v})$, and $\boldsymbol{v}$ is the measurement noise vector.

The error state update equation is as follows

$$\delta \boldsymbol{x} = \boldsymbol{K}(\boldsymbol{y} - h(\boldsymbol{x}, 0))^{-1} \tag{9}$$

The error state covariance update equation of the correction process is as follows

$$\boldsymbol{P} \leftarrow \boldsymbol{P} - \boldsymbol{KHP} \tag{10}$$

Finally, the true state is updated as (4) and the error state is reset since the error of the nominal state has been corrected.

III. NLOS Adaptive Recognition

In the process of signal propagation, some signals cannot be received through the LOS path due to the occlusion of obstacles, which are called NLOS signals. After one or more reflections, the transmission paths of these signals become longer, resulting in large positioning errors, as shown in Figure 2. The signal from BS_1 to the terminal is LOS. But due to obstacles, the signal from BS_2 to the terminal is NLOS. The dotted line will be the propagation path if there is no obstacle. When using d_1 and d_2 for the positioning solution, the error of the positioning result will become larger.

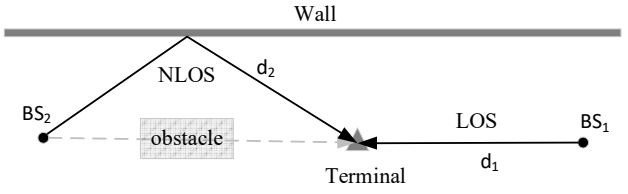

Fig. 2. Formation of NLOS error

Distance measurements can be expressed as follows:

$$d(t) = \begin{cases} d_{real}(t) + \omega_{LOS} & , \ LOS \\ d_{real}(t) + \delta(t) + \omega_{NLOS}, & NLOS \end{cases} \tag{11}$$

where $d_{real}(t)$ is the real distance from the base station to the terminal, $\delta(t)$ is the difference between the NLOS path and the LOS path, ω_{LOS} is the measurement error in the LOS conditions, and ω_{NLOS} is the measurement error in the NLOS conditions. ω_{LOS} and ω_{NLOS} satisfy:

$$\begin{cases} \omega_{LOS} \sim N(0, \sigma_{LOS}^2) \\ \omega_{NLOS} \sim N(0, \sigma_{NLOS}^2) \end{cases} \tag{12}$$

If the signals containing $\delta(t)$ can be identified from the received measurement values, and then these data are eliminated or compensated during the solution, positioning errors will be reduced. In turn, the distance prediction value will be more accurate, and the NLOS signal will be better distinguished. Instead of using the method of recognition based only on the measured values of this epoch, we use a sliding window to record the residuals of a period, and they participate in this recognition together.

In this paper, we propose a recognition method based on timing-optimized GMM clustering. The method mainly consists of three parts, the first part is GMM clustering, the second part is the time sequence optimization of clustering results, and the third part is NLOS recognition.

A. GMM Clustering

Clustering algorithms are unsupervised learning methods. Through learning, we can find groups with common characteristics and classify groups with different characteristics. GMM clustering is accomplished by maximizing the posterior probability. Compared with others such as mean shift clustering, GMM does not need a priori information of mean radius but needs to know the number of classes. Compared with other algorithms that also need the number of classes, such as k-means clustering, GMM gives the probability that all data are assigned to each class, rather than directly assigned to each class.

The principle of GMM is to use multiple Gaussian distribution functions to fit the probability distribution of the data set. These Gaussian distribution functions are added linearly to form the probability density function of the GMM:

$$\begin{aligned} p(x) &= \sum_{k=1}^{K} p(k) p(x|k) \\ &= \sum_{k=1}^{K} \alpha_k p(x|\mu_k, \Sigma_k) \end{aligned} \tag{13}$$

where, K is the number of Gaussian distributions, $p(k)$ and α_k are the probability of the k^{th} Gaussian distribution, $p(x|k)$ is the probability density of the k^{th} Gaussian distribution, which obeys the Gaussian distribution with mean value of μ_k and covariance matrix of Σ_k.

For $d(t)$ in (11), the data can be divided into two categories, LOS cluster and NLOS cluster, by one-dimensional GMM clustering. Suppose the number of data points is L. The clustering process is as follows:

Step 1. Initialize the Gaussian distribution model. Take the mean (μ_1, μ_2) and variance (σ_1, σ_2) of the first half data and the second half data as the initial value of the Gaussian distribution.

1) Step 2. According to the current model parameters, Calculate the posterior probabilities that all data belong to each Gaussian model as (14)

$$\gamma_{ik} = \frac{\alpha_k p(x_i|\mu_k, \sigma_j)}{\sum_{j=1}^{K} \alpha_j p(x_i|\mu_j, \sigma_j)}, i = 1,2,\dots,L; k = 1,2,\dots,K \tag{14}$$

Step 3. Recalculate the parameters of each Gaussian distribution by using the weighting method, as (15)(16)(17). The weights are the probabilities in Step 2.

$$\mu_k = \frac{\sum_{j=1}^{L} \gamma_{jk} x_i}{\sum_{j=1}^{L} \gamma_{jk}} \tag{15}$$

$$\sigma_k = \frac{\sum_{j=1}^{L} \gamma_{jk} (x_i - \mu_k)^2}{\sum_{j=1}^{L} \gamma_{jk}} \tag{16}$$

$$\alpha_k = \frac{\sum_{j=1}^{L} \gamma_{jk}}{L} \tag{17}$$

Step 4. Repeat Step 2 and Step 3 until convergence.

We use the sliding window to store the residual between the predicted value and the measured value in the past certain time period as the data to be clustered. After GMM clustering, the following situations will occur:

2) Only LOS

In this case, the two Gaussian distribution models after the iteration are similar. μ_1 and μ_2 are similar and close to 0. σ_1 and σ_2 are similar, and the discrimination between γ_{i1} and γ_{i2} is small, as shown in Figure 3. The black dots in the left picture are 20 data points collected in a time sequence. The smaller the serial number, the closer to the current time. The black dotted line represents the value 0. The red dotted line represents the mean after convergence of the first Gaussian model. The blue dotted line represents the mean after convergence of the second Gaussian model. The red bar in the picture on the right represents the probability that this point belongs to the first Gaussian model. The blue bar represents the probability that this point belongs to the second Gaussian model.

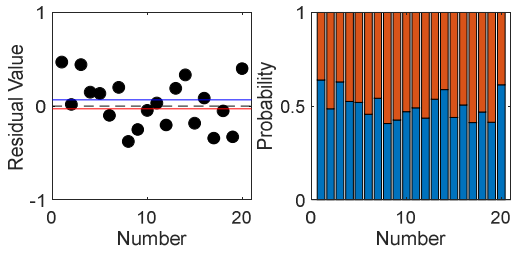

Fig. 3. Clustering results when only LOS exist

3) Both LOS and NLOS

In this case, the two Gaussian distribution models after the iteration are different, μ_1 and μ_2 are different. One of them is close to 0, the other is obviously larger than 0. σ_1 and σ_2 are not necessarily related, and the discrimination between γ_{i1} and γ_{i2} is large, as shown in Figure 4.

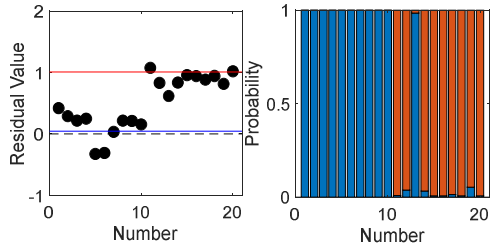

Fig. 4. Clustering results when both LOS and NLOS exist

4) Only NLOS

In this case, the two Gaussian distribution models after the iteration are similar. μ_1 and μ_2 are similar and significantly larger than 0. σ_1 and σ_2 are similar, and the discrimination between γ_{i1} and γ_{i2} is small, as shown in Figure 5.

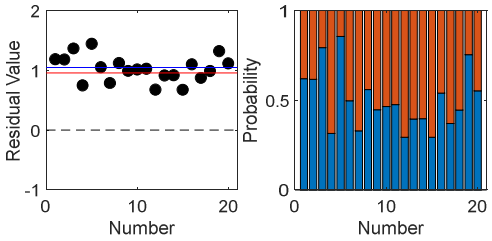

Fig. 5. Clustering results when only NLOS exist

Next, the clustering results γ_{i1} and γ_{i2} are further processed to identify the model that is closer to the current distribution. We introduce a time decay factor λ, use the clustering results to weight λ, and select a Gaussian distribution model with a larger weighted mean as the distribution model at the current moment. The smaller the serial number of the point, the closer to the current moment. The weighted mean of the k^{th} model is

$$\bar{\lambda}_k = \frac{\sum_{j=1}^{L} \gamma_{jk} \lambda^{j-1}}{\sum_{j=1}^{L} \gamma_{jk}} \tag{18}$$

B. Time Sequence Optimization

Since GMM clustering does not consider the sequence of data sampling time, such as the point with the serial number 13 in Figure 4, it is more suitable to be divided into NLOS cluster from the time sequence, but GMM clustering divided it into LOS cluster. This will lead to errors in the mean and variance of the model after clustering. The switching between LOS and NLOS is completed around a certain time, that is, the points in each cluster should maintain time continuity, so it is necessary to optimize the clustering results from the time sequence.

Assuming that the selected cluster serial number is k, we divide γ_k into many intervals and use the mean value of γ_k in the interval as the judgment standard, and select the continuous interval with the mean value greater than 0.5 to form a new cluster. The principle of optimization is shown in Figure 6. The upper part is the GMM clustering before optimization, and the lower part is the clustering after optimization. The cluster is no longer divided by discontinuous points, but by continuous intervals.

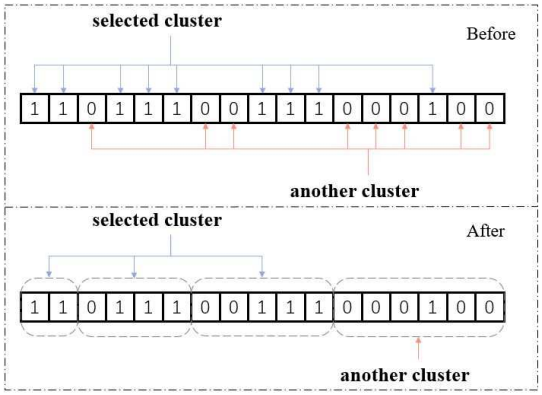

Fig. 6. The principle of time sequence optimization

The specific process of optimization is as follows:

Step 1. Define $Left$ as the left endpoint of the interval to be judged, and the initial value is 1.

Step 2. Find the next point that does not belong to this cluster backward from the current position as the new $Left$.

Step 3. Define $Right$ as the right endpoint of the interval to be judged. $Right$ is the first point found backward from $Left$, which makes the probability that the interval belongs to this cluster higher. $Right$ satisfies

$$\frac{\sum_{j=Left}^{Right}\gamma_{jk}\lambda^{j-1}}{\sum_{j=1}^{L}\gamma_{jk}} > 0.5 \tag{19}$$

If $Right$ can be found, assign the value of $Right$ to $Left$.

Step 4. Repeat Step 2 and Step 3 to find the next interval until the entire sequence is traversed.

Step 5. The points with serial numbers from 1 to $Left$ are used as the optimized cluster.

C. NLOS Recognition

When the signal is always in Los propagation mode, the distance measurement value will change in a small range around the real value of the distance, which is caused by the measurement noise, and there will be no obvious deviation between the two. However, in NLOS propagation mode, in addition to noise, the measured value will have a large deviation from the real value, which is caused by the propagation delay of the signal. The size of this deviation is not fixed, which is affected by the propagation path of the signal. When the terminal is in a dynamic state, the size of the deviation will change.

Our identification method is to detect whether the deviation is within the noise range. If the deviation is within the noise range, it will be identified as LOS. If it is far from the noise range, it will be identified as NLOS. Because the noise range and deviation are given by cluster and are not fixed thresholds, our method is adaptive. The mean represents the deviation and the variance represents the noise range. The weighted mean of the selected cluster by using λ is

$$\hat{\mu} = \frac{1}{Left}\sum_{j=1}^{Left}\lambda^{j-1}x_j \tag{20}$$

The variance is

$$\hat{\sigma}^2 = \frac{1}{Left}\sum_{j=1}^{Left}\lambda^{j-1}(x_j-\hat{\mu})^2 \tag{21}$$

The identification method is

$$\begin{cases}\hat{\mu} \le \hat{\sigma} \Rightarrow LOS\\ \hat{\mu} > \hat{\sigma} \Rightarrow NLOS\end{cases} \tag{22}$$

Signals identified as LOS continue to participate in tight coupling.

IV. Algorithmic Process

This paper proposes a tightly coupled localization method based on NLOS recognition. The algorithm mainly consists of two parts, the first part is initialization and the second part is tight coupling based on NLOS recognition.

A. Initialization

The tight coupling between the ranging signal and the IMU requires the initial position of the terminal, which is used as the initial state to enter the filtering process. The initial position error should not be large, otherwise, it will affect the accuracy of the predicted value. Assuming that in the positioning environment, the terminal can receive the positioning signals transmitted by N base stations. The observed value of the distance from the i^{th} base station to the terminal in the k^{th} time epoch is $d_{i,k}$, and the predicted value is $d_{i,k}^-$. The observation vector before NLOS recognition is

$$\boldsymbol{y}_k = [d_{1,k} \quad d_{2,k} \quad \dots \quad d_{N,k}]^T \tag{23}$$

The distance prediction vector is

$$\boldsymbol{y}_k^- = h(\boldsymbol{x},\boldsymbol{v}) = [d_{1,k}^- \quad d_{2,k}^- \quad \dots \quad d_{3,k}^-]^T \tag{24}$$

Firstly, we use the residual weighted (RWGH) algorithm to perform the TOA solution on $\boldsymbol{y}_1$ at the initial moment to obtain the initial position, which is used to assign the initial state vector $\boldsymbol{x}$.

We build a list of length L as a sliding window to store the residuals between the predicted and measured distances from the base station to the terminal in ESKF. Since each base station must have a list, we use an $N \times L$ matrix for data storage

$$\begin{aligned}\boldsymbol{W} &= [\boldsymbol{y}_k - \boldsymbol{y}_k^- \quad \boldsymbol{y}_{k-1} - \boldsymbol{y}_{k-1}^- \quad \dots \quad \boldsymbol{y}_{k-L+1} - \boldsymbol{y}_{k-L+1}^-]\\ &= \begin{bmatrix}\Delta d_{1,k} & \Delta d_{1,k-1} & \dots & \Delta d_{1,k-L+1}\\ \Delta d_{2,k} & \Delta d_{2,k-1} & \dots & \Delta d_{2,k-L+1}\\ \dots & \dots & \dots & \dots\\ \Delta d_{N,k} & \Delta d_{N,k-1} & \dots & \Delta d_{N,k-L+1}\end{bmatrix}\end{aligned} \tag{25}$$

$$\Delta d_{i,k} = d_{i,k} - d_{i,k}^- \tag{26}$$

Since there is no historical observation at the initial time, the data in $\boldsymbol{W}$ is randomly generated according to the empirical distribution of each observation. We use Gaussian distribution, the mean is 0, and the variance is the empirical value of observation noise σ^2, as

$$\Delta d_{i,j} \sim N(0,\sigma_i^2) \tag{27}$$

B. Tight Coupling Based on NLOS Recognition

After initialization, the algorithm enters the tight coupling. We use the residual between the predicted and the measured distance from the base station to the terminal to identify the NLOS. Because the update frequency of inertial navigation data is higher than that of ranging data, the status correction of ESKF is only performed in the epoch where the ranging data is received. The status prediction is carried out through IMU in all epochs. After the prediction process (5)(6)(7), in the correction process, we calculate $\boldsymbol{y}_k^-$ through (24).

We use $\boldsymbol{y}_k$ and $\boldsymbol{y}_k^-$ to update $\boldsymbol{W}$ by (25), then perform NLOS recognition on the N rows of data of $\boldsymbol{W}$. According to the recognition results, n LOS observations will be selected, and the observations will be reconstructed as follows

$$\hat{\boldsymbol{y}}_k = [d_{1,k} \quad d_{2,k} \quad \dots \quad d_{n,k}]^T \tag{28}$$

Correspondingly, we also reconstruct $\boldsymbol{H}$ in (8).

Affected by the complex environment and NLOS noise, the measurement noise received by the terminal will change in real-time, so the observation noise covariance matrix $\boldsymbol{R}$ cannot be given empirically. The weighted variance in (21) can be adjusted according to the residual distribution, which can be used to optimize $\boldsymbol{R}$. The way to improve is as follows

$$\boldsymbol{R} = diag\{\hat{\sigma}_1^2, \hat{\sigma}_2^2, \dots, \hat{\sigma}_n^2\} \tag{29}$$

where $\hat{\sigma}_1^2$ is the variance of the i^{th} group of residuals in the identification process.

After the above optimization is completed, continue to perform (8) (9) (10) to complete the correction process.

The following chart shows the detailed progress of our algorithm.

Algorithm: Tight coupling based on NLOS recognition

Input: The coordinates of base station $[x_i, y_i, z_i], i = 1,2, \dots, N$, the observation of distance $\boldsymbol{y}_k$, acceleration $\boldsymbol{a}_m$, and angular velocity $\boldsymbol{\omega}_m$ provided by IMU

Output: the location of the terminal $[x_k, y_k, z_k]$

START

1. Prediction process, use $\boldsymbol{a}_m$ and $\boldsymbol{\omega}_m$ to update $\boldsymbol{x}$ and $\boldsymbol{P}$
2. IF there is observation $\boldsymbol{y}_k$ in this epoch
3. Calculate prediction $\boldsymbol{y}_k^-$, update $\boldsymbol{W}$
4. FOR $i = 1$ TO N
5. Perform GMM clustering on $\boldsymbol{W}_i$, and perform time sequence optimization and NLOS recognition on the selected cluster.
6. Select n LOS observations, construct $\hat{\boldsymbol{y}}_k$
7. Correction process, calculate $\boldsymbol{H}$ and $\boldsymbol{R}$
8. Update $\delta\boldsymbol{x}$ and $\boldsymbol{P}$
9. Update the true state $\boldsymbol{x}_t$
10. ENDIF
11. Get the positioning result $\boldsymbol{p}$ of this epoch

END

V. Simulation and Practical Testing

In order to verify the performance of our proposed algorithm, we have carried out simulations and practical tests and compared the performance of our NLOS recognition algorithm and location algorithm with other methods.

The experimental scene is in the atrium on the first floor of the scientific research building of the Beijing University of Posts and Telecommunications, as shown in Figure 7 (a). The test is divided into static test and dynamic test. The former is used to evaluate the NLOS recognition performance, and the latter is used to evaluate the positioning algorithm. The UWB model used in the experiment is dw1000, and the data sampling frequency is 5Hz. The model of IMU is mpu9250, and the data sampling frequency is 50Hz. The equipment photo is shown in Figure 7 (b). The base station is above and the positioning terminal is below. The base stations broadcast UWB signals, and the terminal integrates INV and UWB.

(a) experimental environment (b) base stations and terminal

Fig. 7. Experimental conditions

A. NLOS Recognition Evaluation

This evaluation is performed while the terminal remains static. Los data and NLOS data are collected by the UWB module. The terminal and base station are in the LOS state at first, and later become NLOS due to occlusion. We used K-means clustering, GMM clustering, and time series optimized GMM clustering (TGMM) to process the collected data. The collected data contains both NLOS and Los. We selected 100 consecutive sampling points in the collected data. By adjusting the ratio of NLOS data and LOS data in the sampling points, we analyze the feature resolution ability of the three methods for the data. Repeat the experiment 100 times under the same conditions, and take the average value. The time decay factor λ takes a value of 0.95. The performance indicator is the clustering success rate, which is defined as the ratio of the number of successfully divided data points to the total number.

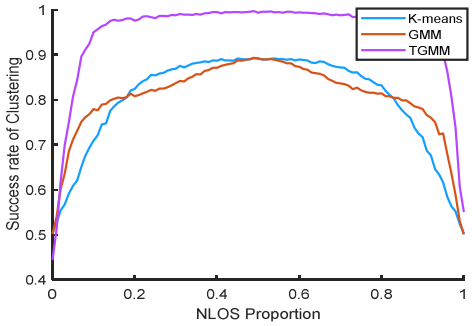

Fig. 8. Performance of different clustering algorithms

The clustering performance is shown in Figure 8. The abscissa axis is the proportion of NLOS in the mixed data, the number of sampling points is fixed at 100, and the ordinate axis is the success rate. It can be seen from the figure that all methods have the best performance when the proportion of NLOS data is 50%, and the success rates of other proportions are symmetrically distributed. Compared with K-means clustering, GMM clustering has a more sensitive data discrimination ability. Higher sensitivity can help the algorithm more quickly identify whether the model of the time series has changed. However, when the proportion of the two kinds of data is close, the GMM clustering ability is not as good as K-means clustering. TGMM clustering performs best, both in terms of sensitivity and success rate under the same data. In most cases, the success rate of TGMM remains above

97%, while K-means and GMM only maintain 88% in the best cases.

Because TGMM method introduces the time decay factor λ, we conducted simulation experiments for different λ under different constituted datasets to see the impact on the recognition. LOS distribution model is set to $N(0, 0.2^2)$, and the unit is meters. NLOS distribution model is set to $N(0.4, 0.2^2)$, and the unit is meters. The total number of points is 100, consisting of LOS data and NLOS data. NLOS data has a smaller time sequence number. We changed the composition of the dataset by controlling the proportion of NLOS data in the dataset to see whether the algorithm can recognize NLOS. Each configuration is independently repeated 1000 times.

The simulation test results are shown in Figure 9, in which the success rate of judgment is the number of successful recognitions divided by the total number of tests. The value of the time decay factor λ ranges from 0.6 to 1. If λ is too small, NLOS recognition will be more dependent on the data of the most recent epoch, and the weight of other data in the sequence will be too small and lose statistical significance. Combined with the color bar, in most cases, λ in the range of $0.6\sim1$ can make the recognition success rate greater than 0.95, which has good robustness. The red area of the surface is concentrated in the range where λ above 0.8, it can maintain a success rate of more than 99%, indicating that a larger λ will make the algorithm have higher accuracy. However, a larger λ also has a negative impact. From (20), if λ is larger, the weight advantage of points with a small sequence number will be reduced. This will lead to a decrease in the sensitivity of the algorithm. It can also be seen from the image. In the face of the small proportion of NLOS data, the performance of a larger λ is not as good as that of a smaller λ.

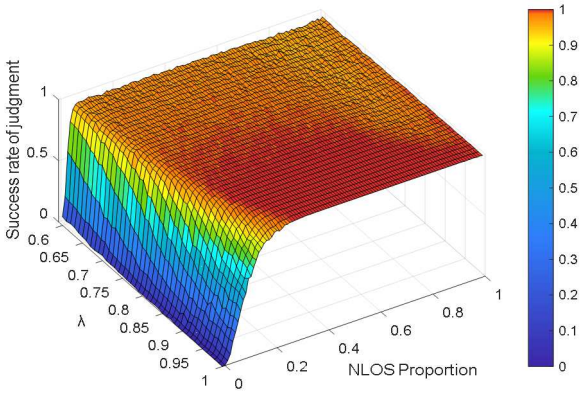

Fig. 9. Test of NLOS recognition performance

In the above simulation experiments, we also observed the fitting ability of TGMM algorithm to the NLOS distribution model, and the results are shown in Figure 10. The data on the contour line is the root mean square error of the parameter estimation, in meters. The error statistics for the parameter μ are in the left figure, and the error statistics for the parameter σ are in the right figure. In most cases, when λ is larger, the fitted model is more accurate. The fitting results are also subject to the proportion of NLOS data. The less NLOS data, the lower the fitting accuracy. The fitting result is consistent with the recognition result in Figure 9. The higher the fitting parameter precision, the more accurate the recognition. The disadvantage is that the sensitivity is reduced. Therefore, TGMM chooses a λ greater than 0.9 when localizing.

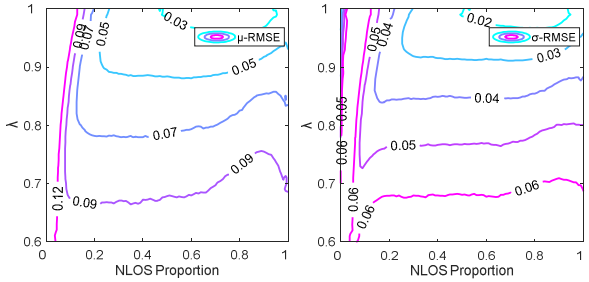

Fig. 10. Fitting accuracy performance of TGMM

B. *Localization Algorithm Evaluation*

The evaluation is performed while the terminal remains in motion. Figure 7 (a) shows the real environment. Figure 11 shows the distribution of base stations. Four base stations are deployed on the first floor, marked as $BS_{1\sim4}$. The other four base stations are arranged on the second floor, marked as $BS_{5\sim8}$. The base station on the second floor is close to the edge of the atrium, so the transmitted signal can be received by the terminal on the first floor. The area they enclose is the extent of the atrium. The terminal always keeps a certain height and moves on the first floor. The moving route is the orange line in the map. The small square in the figure represents the floor tiles in the lobby. The terminal uses the floor tiles as a reference when moving, and passes a floor tile every 2 seconds. The gray area is also located on the first floor but has left the atrium area, and the ranging signal will receive severe NLOS interference. The purple area is the load-bearing column.

Select base station 3 as the origin, and the distance unit is meters. The positions of the eight base stations are BS_1 (12.62, 7.57, 0), BS_2 (12.62, 0, 0), BS_3 (0, 0, 0), BS_4 (0, 7.57, 0), BS_5 (15, 9.97, 4.83), BS_6 (15, -1.3, 4.83), BS_7 (-1.68, -1.3, 4.83), BS_8 (-1.68, 9.97, 4.83). The terminal start position is (5.89, 0.84, 1.6). The end position is (-4.21, 1.68, 1.6).

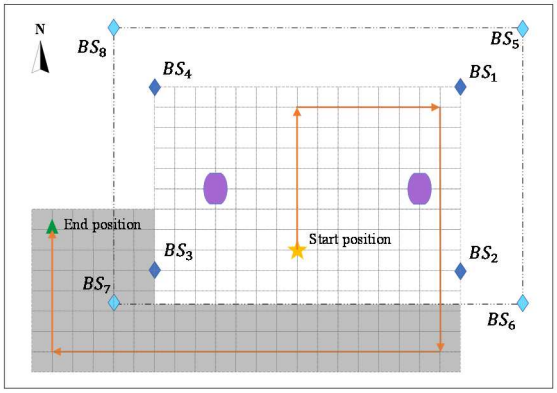

Fig. 11. Schematic diagram of the terminal motion experiment scene

Besides the proposed algorithm, we also use other algorithms for testing, as shown in Table 1. These algorithms are compared according to the coupling mode and whether they can reduce NLOS error.

TABLE I. LOCATION ALGORITHM

Name	Coupling mode	NLOS processing	denoted
Chan algorithm	No coupling	No	Chan
Residual weighting algorithm	No coupling	Yes	RWGH

Name	Coupling mode	NLOS processing	denoted
Combined positioning of RWGH and IMU based on ESKF	Loose coupling	Yes	RWGH-ESKF
Combined positioning of RWGH and IMU based on particle filter	Loose coupling	Yes	RWGH-EPF
Combined positioning of distance measurement and IMU based on adaptive filtering	Tight coupling	No	SageHusa-KF

After eliminating the system error, the two-dimensional positioning error is shown in Figure 12. Because the terminal remains a certain height, we analyze the positioning effect on the plane. When the terminal passes through the load-bearing column on the right side of Figure 11, between 34th and 40th seconds in Figure 12, there are obvious errors in the solution result. Because the four base stations BS_3, BS_4, BS_7, and BS_8 are occluded, the observations have NLOS errors. After 48 seconds, the terminal enters the gray area in Figure 11, BS_6 and BS_7 become NLOS base stations, which have a greater impact on the positioning. Compared with other algorithms, our algorithm has smaller error. The average error of Chan is 1.71m. The average error of RWGH is 0.96m. The average error of RWGH-ESKF is 0.94m. The average error of RWGH-EPF is 0.94m. The average error of SageHusa-KF is 0.81m. The average error of Proposed is 0.43m. The accuracy is 47% higher than traditional tight coupling.

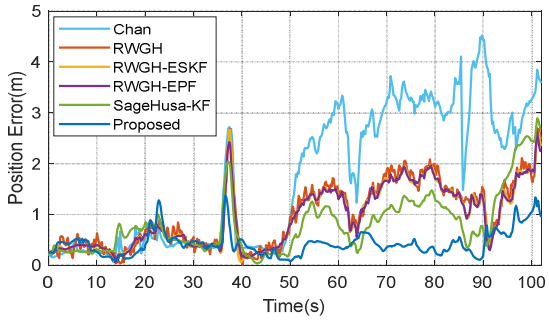

Fig. 12. Plane positioning error

After the introduction of IMU, the loosely coupled localization algorithm is smoother than RWGH, but there is no significant improvement in the error caused by NLOS. Tight coupling further reduces the positioning error, but it has no special treatment for NLOS error. Based on tight coupling, our algorithm selects the appropriate ranging value through NLOS recognition, which can improve the positioning accuracy in complex environments. The error cumulative distribution is shown in Figure 13.

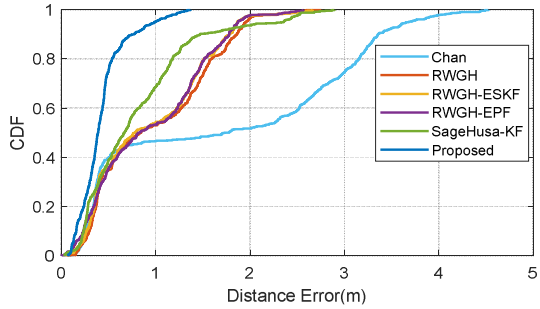

Fig. 13. Error accumulation distribution of various positioning algorithms

VI. Conclusions

In this paper, we propose a new NLOS recognition method and use it for tightly coupled localization of ranging signals and IMU. The method uses ESKF to predict the distance between the terminal and base stations, and judges whether there is an NLOS error through the residual difference between the predicted value and the measured value. In order to improve the recognition performance of NLOS and LOS mixed data, a time series optimized GMM clustering method is proposed. Compared with other methods, the residual distribution model obtained by this clustering method is more accurate. We have conducted practical tests using UWB and IMU, and our method improves the accuracy by 47%. The limitation of the algorithm is that the initial positioning environment cannot be too harsh, otherwise, it will affect the NLOS recognition, which is the next problem we will study.

Acknowledgment

This work was supported by the National Key Research and Development Program of China(No. 2020YFC1511702).

References

[1] X. Guo, N. Ansari, F. Hu, Y. Shao, N. R. Elikplim, and L. Li, "A Survey on Fusion-Based Indoor Positioning," *IEEE Communications Surveys & Tutorials*, vol. 22, no. 1, pp. 566-594, 2020.

[2] S. Gezici and H. V. Poor, "Position Estimation via Ultra-Wide-Band Signals," *Proceedings of the IEEE*, vol. 97, no. 2, pp. 386-403, 2009.

[3] X. Yang, J. Wang, D. Song, B. Feng, and H. Ye, "A Novel NLOS Error Compensation Method Based IMU for UWB Indoor Positioning System," *IEEE Sensors Journal*, vol. 21, no. 9, pp. 11203-11212, 2021.

[4] L. Jiao, J. Xing, X. Zhang, J. Zhang, and C. Zhao, "LCC-Rwgh: A NLOS Error Mitigation Algorithm for Localization in Wireless Sensor Network," in *2007 IEEE International Conference on Control and Automation*. 2007, pp. 1354-1359.

[5] Wang L, Chen R, Shen L, Qiu H, Li M, Zhang P, Pan Y, "NLOS Mitigation in Sparse Anchor Environments with the Misclosure Check Algorithm." *Remote Sensing*, vol. 11, no. 7, p. 773, 2019.

[6] Q. Shi, S. Zhao, X. Cui, M. Lu, and M. Jia, "Anchor self-localization algorithm based on UWB ranging and inertial measurements," *Tsinghua Science and Technology*, vol. 24, no. 6, pp. 728-737, 2019.

[7] Z. Zeng, S. Liu, and L. Wang, "NLOS Detection and Mitigation for UWB/IMU Fusion System Based on EKF and CIR," in *2018 IEEE 18th International Conference on Communication Technology (ICCT)*. 2018, pp. 376-381.

[8] Y. Wang and X. Li, "The IMU/UWB fusion positioning algorithm based on a particle filter," *ISPRS International Journal of Geo-Information*, vol. 6, no. 8, p. 235, 2017.

[9] L. Cheng, X. Wu, and Y. Wang, "A non-line of sight localization method based on k-means clustering algorithm," in *2017 7th IEEE International Conference on Electronics Information and Emergency Communication (ICEIEC)*. 2017, pp. 465-468.

[10] F. Wu and Z. Liu, "Research on UWB / IMU Fusion Positioning Technology in Mine," in *2020 International Conference on Intelligent Transportation, Big Data & Smart City (ICITBS)*. 2020, pp. 934-937.

[11] W. Guosheng, Q. Shuqi, L. Qiang, W. Heng, L. Huican, and L. Bing, "UWB and IMU System Fusion for Indoor Navigation," in *2018 37th Chinese Control Conference (CCC)*. 2018, pp. 4946-4950.

[12] N. Wang, X. Yuan, L. Ma, and X. Tian, "Research on Indoor Positioning Technology Based on UWB," in *2020 Chinese Control And Decision Conference (CCDC)*. 2020, pp. 2317-2322.

[13] J. He, C. Sun, B. Zhang, and P. Wang, "Adaptive Error-State Kalman Filter for Attitude Determination on a Moving Platform," *IEEE Transactions on Instrumentation and Measurement*, vol. 70, no. 1, pp. 1-10, 2021.